

2

DTIC DOCUMENTATION PAGE				
1a. REPORT SECURITY CLASSIFICATION Unclassified		1b. RESTRICTIVE MARKINGS DTIC FILE COPY		
2a. SECURITY CLASSIFICATION AUTHORITY DEC 06 1988		3. DISTRIBUTION/AVAILABILITY OF REPORT Approved for public release; distribution unlimited.		
AD-A202 464		5. MONITORING ORGANIZATION REPORT NUMBER(S) ARO 22929.3-CH		
6a. NAME OF PERFORMING ORGANIZATION University of Wisconsin		6b. OFFICE SYMBOL (If applicable)		7a. NAME OF MONITORING ORGANIZATION U. S. Army Research Office
6c. ADDRESS (City, State, and ZIP Code) 1101 University Ave. Madison, WI 53706		7b. ADDRESS (City, State, and ZIP Code) P. O. Box 12211 Research Triangle Park, NC 27709-2211		
8a. NAME OF FUNDING/SPONSORING ORGANIZATION U. S. Army Research Office		8b. OFFICE SYMBOL (If applicable)		9. PROCUREMENT INSTRUMENT IDENTIFICATION NUMBER DAA629-85-K-0122
8c. ADDRESS (City, State, and ZIP Code) P. O. Box 12211 Research Triangle Park, NC 27709-2211		10. SOURCE OF FUNDING NUMBERS PROGRAM ELEMENT NO. PROJECT NO. TASK NO. WORK UNIT ACCESSION NO.		
11. TITLE (Include Security Classification) Time and State Resolved Studies of Molecular Decomposition				
12. PERSONAL AUTHOR(S) F. Fleming Crim				
13a. TYPE OF REPORT Final		13b. TIME COVERED FROM 8/1/85 TO 7/31/88		14. DATE OF REPORT (Year, Month, Day) 1988, October, 17
15. PAGE COUNT 23				
16. SUPPLEMENTARY NOTATION The view, opinions and/or findings contained in this report are those of the author(s) and should not be construed as an official Department of the Army position, policy, or decision, unless so designated by other documentation.				
17. COSATI CODES FIELD GROUP SUB-GROUP			18. SUBJECT TERMS (Continue on reverse if necessary and identify by block number) molecular decomposition, vibrational excitation, photodissociation, MOLECULAR PROPERTIES. (JES)	
19. ABSTRACT (Continue on reverse if necessary and identify by block number) Molecular decompositions often control complex chemical reactions by producing a highly reactive fragment that determines the subsequent chemistry. Despite the importance of such processes, there is little detailed information available for testing theoretical models and guiding the analysis of practical systems. This report describes experiments that produce, characterize, and dissociate highly energized molecules in order to uncover the details of molecular decomposition. These experiments are able to explore decompositions solely in the ground electronic state by vibrational overtone induced dissociation, to investigate the role of vibrational excitation in electronic photodissociation using vibrationally mediated photodissociation, and to identify primary fragments and determine the kinetic energy release in electronic photodissociation using energy selective ionization.				
20. DISTRIBUTION/AVAILABILITY OF ABSTRACT <input type="checkbox"/> UNCLASSIFIED/UNLIMITED <input type="checkbox"/> SAME AS RPT. <input type="checkbox"/> DTIC USERS			21. ABSTRACT SECURITY CLASSIFICATION Unclassified	
22a. NAME OF RESPONSIBLE INDIVIDUAL			22b. TELEPHONE (Include Area Code)	22c. OFFICE SYMBOL

FINAL REPORT

Time and State Resolved Studies of Molecular Decomposition

(DAAG29-85-K-0122)

Abstract

Molecular decompositions often control complex chemical reactions by producing a highly reactive fragment that determines the subsequent chemistry. Despite the importance of such processes, there is little detailed information available for testing theoretical models and guiding the analysis of practical systems. This report describes experiments that produce, characterize, and dissociate highly energized molecules in order to uncover the details of molecular decomposition. These experiments are able to explore decompositions solely in the ground electronic state by vibrational overtone induced dissociation, to investigate the role of vibrational excitation in electronic photodissociation using vibrationally mediated photodissociation, and to identify primary fragments and determine the kinetic energy release in electronic photodissociation using energy selective ionization.

Introduction

Our work supported by the Army Research Office (DAAG29-85-K-0122) has been directed toward producing, characterizing, and dissociating highly energized molecules. Our production of highly vibrationally excited molecules uses one-photon excitation of overtone vibrations, and we have employed this excitation for vibrational overtone induced dissociation in several molecules in both room-temperature gases and in cold supersonic expansions in order to determine unimolecular reaction rates and product energy partitioning. We have also developed the technique of vibrationally mediated photodissociation, in which we electronically photodissociate a highly vibrationally excited molecule, both as a means of characterizing initially prepared vibrational states and of producing unique electronic photodissociation dynamics. In a somewhat different approach, we have implemented an energy-selective electron impact ionization scheme for identifying the primary products of a dissociation and measuring their kinetic energy. This report describes our work in each of these three areas along with the approaches we have developed.

Vibrational Overtone Induced Dissociation

We have studied the vibrational overtone induced dissociation of several molecules ranging from the small tetra-atomic and penta-atomic molecules $\text{HOOH}^{1,2,3}$ and HONO_2^4 to very large species



Availability Codes	
Dist	Avail and/or Special
A-1	

such as tetramethyldioxetane,⁵ which contains 20 atoms. In these experiments, we prepare a highly vibrationally excited molecule by laser excitation of an overtone vibration and then interrogate the products spectroscopically using either product chemiluminescence^{5,6} or laser induced fluorescence.¹⁻³ The latter technique determines the population of individual product quantum states as well as providing rate information.

We have taken two approaches to determining the unimolecular reaction rates of molecules with excited overtone vibrations. One is quite direct in that we spectroscopically monitor the appearance of reaction products as a function of time. Because the 10 ns duration of our laser pulses determines the time resolution of this method, we apply it to large molecules whose unimolecular reaction rates are slow enough to be resolved.⁵ Our second approach is a more inferential scheme in which we attempt to observe single, homogeneous lines in a vibrational overtone spectrum and determine the unimolecular reaction rate from the widths of these features.³ This technique is complementary to the first since it is best applied to small molecules that react so rapidly that the resulting linewidth substantially exceeds our limiting laser resolution of about 0.05 cm^{-1} . Performing both experiments on molecules cooled in a free jet expansion is an important aspect of our approach since it reduces the distribution of initial thermal energies in large molecules⁶ and provides the spectral simplification required to observe isolated features in small molecules.³

Direct Measurements. - The energy level diagram in Fig. 1 illustrates the application of our technique to tetramethyldioxetane (TMD). Excitation in the regions of the two overtone transitions $4\nu_{\text{CH}}$ and $5\nu_{\text{CH}}$ and of the combination band $4\nu_{\text{CH}} + \nu_{\text{def}}$ adds sufficient energy to the molecule for it to decompose to produce electronically excited acetone. Observing the time evolution of the emission from the chemiluminescent product is a means of monitoring the progress of the vibrational overtone initiated dissociation directly. We know the added energy is that of the photon $h\nu$ but have no control over the amount of thermal excitation that a particular molecule possesses in experiments in

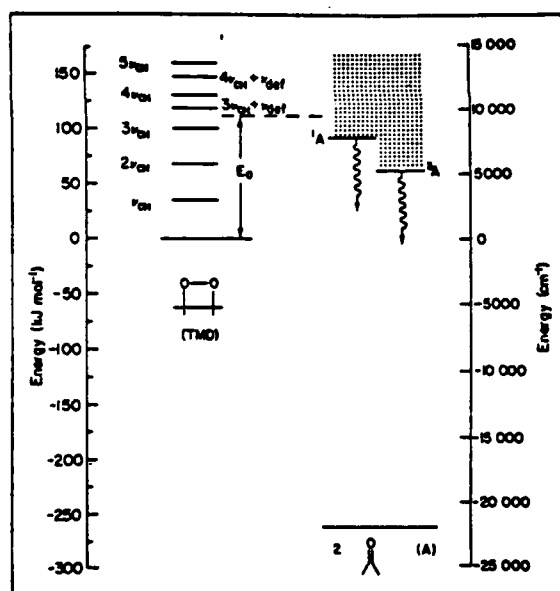


Figure 1

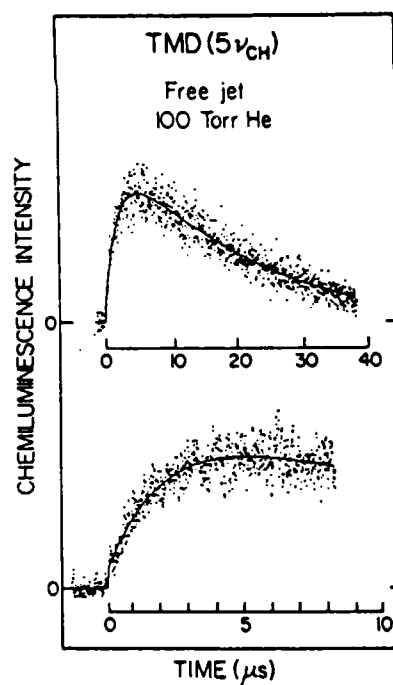


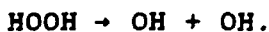
Figure 2

room-temperature gases. Consequently, we must average any theoretical calculation for comparison with experiment. We overcome this limitation by inducing the decomposition in a supersonic expansion where the range of initial energies is quite small.

Figure 2 shows the time-evolution of products from the vibrational overtone induced decomposition of TMD in a free-jet expansion. The growth of products reflects the unimolecular dissociation rate, which we extract from the data by means of the fit that is shown as a solid curve. This reaction rate of $0.52 \pm 0.10 \mu\text{s}^{-1}$ is the point of comparison with a statistical (RRKM) theory of unimolecular reactions. We are able to reproduce this value with a RRKM calculation⁵ and, most important, are able to use that calculation to describe all of the room-temperature vibrational overtone induced dissociation data for excitation of the $4\nu_{\text{CH}}$, $3\nu_{\text{CH}} + \nu_{\text{def}}$, and $5\nu_{\text{CH}}$ vibrational overtone transitions.⁵

Indirect Measurements. - The spectrum of the $6\nu_{\text{OH}}$ vibrational overtone region for hydrogen peroxide molecules cooled in a supersonic expansion, shown in Fig. 3(e), is the means by which we infer the dissociation rate of that excited molecule. Figure 4 shows the energetics for the vibrational overtone induced decomposition [Figure 4(a) and 4(b)] as well as those for the vibrationally mediated mediated photodissociation to be discussed below [Figure 4(c) and 4(d)]. The decomposition of hydrogen peroxide requires about 210 kJ mol^{-1} of energy and produces two OH

fragments that we detect by laser induced fluorescence



The width of the features in the region of the $6\nu_{\text{OH}}$ transition, which excites the HOOH above its dissociation threshold, is

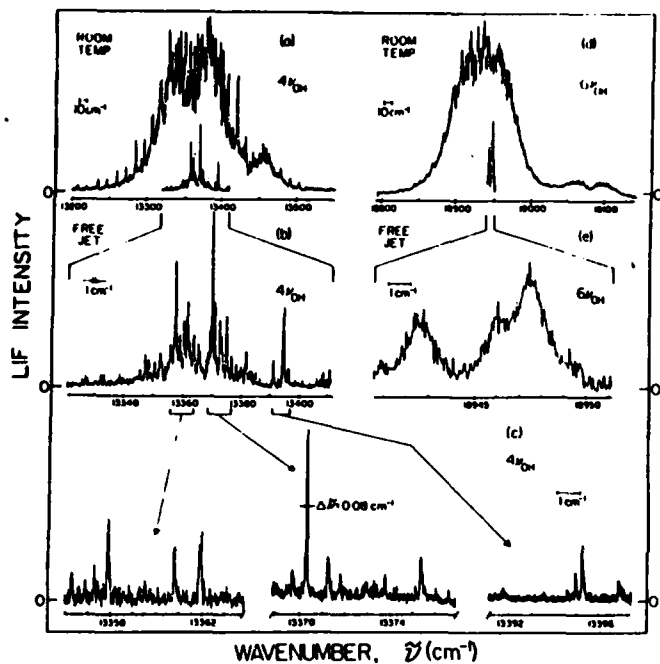


Figure 3

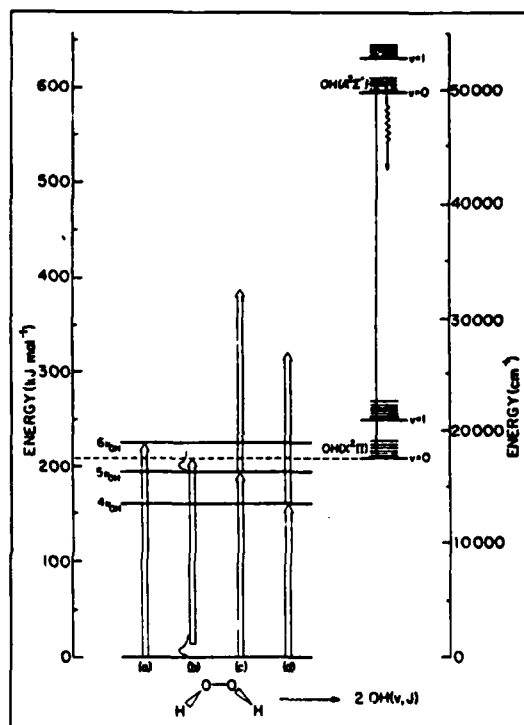


Figure 4

significantly greater than that of features in the region of the $4\nu_{\text{OH}}$ [Figure 3(c)] transition, which adds too little energy to dissociate the molecule. If the $1.5 \pm 0.3 \text{ cm}^{-1}$ width of the feature at $18,942.5 \text{ cm}^{-1}$ arises entirely from coupling into the continuum, the dissociation lifetime is $\tau = 3.5 \text{ ps}$, corresponding to an upper limit to the rate constant of $k = 2.9 \times 10^{11} \text{ s}^{-1}$. Because the cooling in the supersonic expansion ensures that the HOOH molecules have a total energy equal to the photon energy and that

they possess very little angular momentum, the measurement approaches a determination of the detailed rate constant $k(E,J)$ required for the most complete comparison to the predictions of statistical theories.

The rate constant inferred from the linewidth is consistent with two rather different calculations of the lifetime of $\text{HOOH}(6\nu_{\text{OH}})$. It agrees with both a statistical calculation,^{2,10} which assumes complete energy redistribution, and a trajectory calculation,¹¹ which finds that energy randomization is incomplete. Determining the limits of applicability of statistical models in hydrogen peroxide requires other diagnostics of the dynamics of the decomposition process, and the product state distributions for HOOH cooled in a free jet expansion are likely to be helpful in this regard.

Product State Distributions. - The distribution of the products of a photodissociation among their quantum states is potentially a sensitive probe of the decomposition dynamics. Our measurements of the populations of the rotational states of the OH product of the vibrational overtone initiated decomposition of hydrogen peroxide and of nitric acid are a means of comparing different statistical theories of unimolecular decomposition.

The distributions of products of the dissociation of HOOH among their rotational states for excitation near threshold ($5\nu_{\text{OH}}$) and well above threshold ($6\nu_{\text{OH}}$) differ substantially. Figure 5 collects the experimental results (solid bars) for excitation in the region of the two transitions.^{2,12} The lowest rotational

state is the most highly populated for fragments produced by excitation in the region of the $5\nu_{\text{OH}}$ transitions, but the most populated rotational state in the fragments produced by excitation in the region of the $6\nu_{\text{OH}}$ transition is about $N = 4$ or 5. We have used these distributions for comparisons with two statistical theories of unimolecular decomposition, phase space theory¹³ (PST) and the statistical adiabatic channel model¹⁴ (SACM). Both models explicitly conserve energy and angular momentum, but differ in their treatment of the interaction potential between the

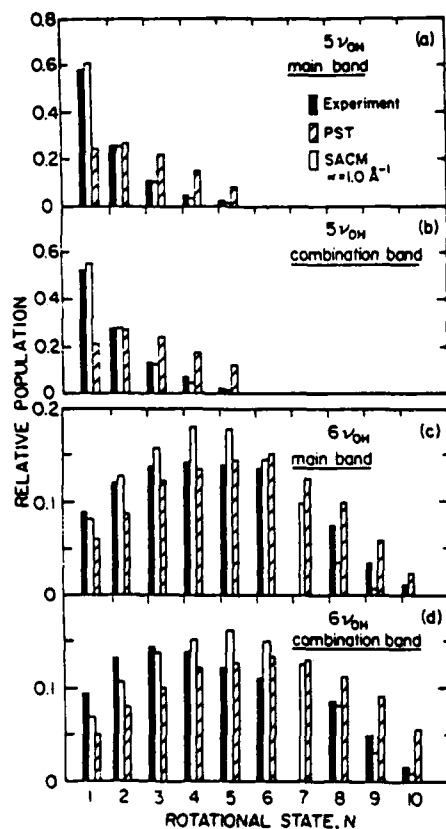


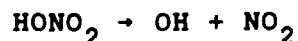
Figure 5

separating fragments. This causes the statistical adiabatic channel model to predict less rotational excitation in the

products than does the phase space theory.¹⁰

As Figure 5 shows, both the phase space theory (hatched bars) and the statistical adiabatic channel model (open bars) predict qualitatively similar distributions of products following excitation in the $6\nu_{\text{OH}}$ region, but the situation is drastically different for excitation of transitions in the $5\nu_{\text{OH}}$ region. The SACM prediction agrees with the experimental results quite well, but phase space theory predicts substantially more rotational excitation than we observe experimentally. This comparison of the calculations and measurements is an example of the success of the statistical adiabatic channel model in a situation where phase space theory is inadequate and, most important in the present context, demonstrates how product state distributions permit clear distinctions between statistical theories.

Our recent study of the vibrational overtone induced decomposition of nitric acid⁴



following excitation in the regions of the $5\nu_{\text{OH}}$ and $6\nu_{\text{OH}}$ transitions further illustrates the utility of measuring product state distributions for comparison to theory.¹⁵ The distributions are qualitatively similar to those for HOOH at the two levels of excitation, and phase space theory fails in a similar manner. We are currently performing statistical adiabatic channel model calculations to complete the comparison. These observations for HOOH and HONO₂ are particularly interesting in light of recent photofragment measurements of product state distributions for ketene on the ground singlet surface by Moore and coworkers.¹⁶

They find the PST describes their results well while the SACM using the standard parameter is inadequate. Wittig and coworkers^{15,17} have previously drawn similar conclusions about NCNO decomposition with small excess energies. The challenge is to understand the features that distinguish systems that satisfy PST from those that satisfy the SACM.

Vibrationally Mediated Photodissociation

The schematic drawing of a ground state potential energy surface and a repulsive electronically excited surface shown in Figure 6 illustrates vibrationally mediated photodissociation for a HOX molecule. (In our applications to date, X is OH,³ NO₂¹⁸, and t-BuO¹⁹.) This diagram shows the surfaces along the bound stretching coordinate (the OH stretching vibration) and the dissociative coordinate (the OX stretching vibration). The OH vibration is bound in both the ground and electronically excited states, but the OX vibration is unbound in the latter. Conventional photodissociation excites a molecule from a region near the minimum on the lower surface to the repulsive upper surface, but the two-step vibrationally mediated photodissociation process first excites a high vibrational level of the ground electronic state and, subsequently, dissociates the vibrationally excited molecule with a second photon. Thus, the dissociation occurs from a rather different part of the ground state potential energy

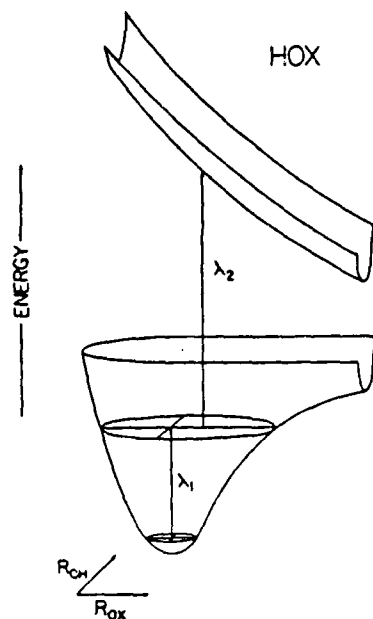


Figure 6

surface than does the usual one-photon process. The energies of the excitation photon (λ_1) and dissociation photon (λ_2) shown in Figure 6 are each insufficient to dissociate the molecule from its equilibrium geometry, and the dissociation by the second photon must occur from a region in which the extension of the OX coordinate brings the ground and excited electronic surfaces closer than in the equilibrium configuration. Vibrationally mediated photodissociation allows us to assess the nature of the state prepared by vibrational overtone excitation and to observe differences in the electronic dissociation dynamics of vibrationally excited molecules. Both types of information come from the participation of usually inaccessible parts of the ground and electronically excited potential energy surfaces in the vibrationally mediated photodissociation.

Vibrational Overtone Spectroscopy. - An extension of the local mode model using a zero-order state, which carries the oscillator strength for the transition, coupled to background states²⁰⁻²¹ provides an extremely useful connection between spectral observations and couplings within a molecule. A central goal of our vibrational overtone spectroscopy is obtaining a description of the initially excited state as an admixture of zero-order states about which one has good chemical intuition. This is possible using vibrationally mediated photodissociation because the intensities of the transitions reflect the degree to which motion along the dissociation coordinate (OX) is coupled with the local mode vibration corresponding to the zero-order state carrying the transitions strength (OH stretching). Because only those initial states that have a significant amount of OX stretching character can absorb the dissociation photon for the energetic situation illustrated in Figure 6, the production of fragments signals the participation of the zero-order OX stretching state. Varying the vibrational overtone excitation wavelength (λ_1) produces an excitation spectrum of those molecules that absorb a second photon to dissociate to yield a fragment in the probed product state. The room temperature and free jet spectra for $\text{HOOH}(4\nu_{\text{OH}})$ (Figure 3) obtained by this scheme demonstrate the utility of vibrationally mediated photodissociation as a spectroscopic technique.

Photofragment Product State Distributions. - We measure the distribution of the OH products of vibrationally mediated photodissociation among their quantum states by laser induced fluorescence and determine the product recoil energy from the Doppler widths of the probe transitions. For hydrogen peroxide, this allows us to assess the energy disposal completely while we can only infer the internal energy of the other fragment for nitric acid ($X=\text{NO}_2$) and t-butylhydroperoxide ($X=\text{t-BuO}$). The larger NO_2 and t-BuO fragments from nitric acid and t-butylhydroperoxide acquire a considerably greater fraction (78% and 89%, respectively) of the available energy as internal excitation than do the OH fragments from hydrogen peroxide, which obtain only 29% of the total. The large amount of average internal energy ($19\,500\text{ cm}^{-1}$) in the NO_2 fragment suggests excitation of its low lying electronic states, a possibility that we plan to explore.

The production of vibrationally excited fragments in the vibrationally mediated decomposition of HOOH and HONO_2 reflects a striking change in the dissociation dynamics compared to the case of one-photon ultraviolet dissociation. Ultraviolet dissociation of hydrogen peroxide at $\lambda=355\text{ nm}$,²² 266 nm ,²³ 248 nm ,^{24,25} and even 193 nm ²⁶ produces no vibrationally excited OH fragments compared to 10% to 20% for the vibrationally mediated process, depending on the energy of the dissociating photon (λ_2). (The vibrationally mediated photodissociations use either $\lambda_1=\lambda_2=750\text{ nm}$ or $\lambda_1=750\text{ nm}$ and $\lambda_2=532\text{ nm}$). The enhanced vibrational excitation is not an energetic effect, since the ultraviolet excitation adds a larger amount of energy, but rather arises from the vibrational

excitation influencing the dynamics of the dissociation. Nitric acid behaves similarly in that vibrationally mediated photodissociation produces about 5% vibrationally excited OH fragments^{18,19,27} compared to none in the case of 280 nm one-photon dissociation.²⁸

Energy Selective Electron Impact Ionization

We have recently demonstrated a scheme in which we use energy selective electron impact ionization to identify the primary products of an electronic photodissociation and to measure the kinetic energy released into the fragments²⁹. The first application is the most important in the context of this proposal, and the following briefly describes the approach in general along with its application to the dissociation of methyl iodide (CH_3I).

The completion of our molecular beam apparatus for these studies has been an important activity during this period of Army Research Office support, and the success of these new experiments reflects that effort. The apparatus consists of a separately pumped source that produces a skimmed, pulsed molecular beam that enters a differentially pumped time-of-flight mass spectrometer. The heart of the energy selective ionization experiments is a pulsed, low-energy electron gun that produces space charge limited currents at energies as low as a few eV with an energy distribution characterized by $T \approx 1300 \text{ K}$ ($2kT = 0.2 \text{ eV}$).^{30,31} (The large ionizer of the mass spectrometer is also designed to accommodate laser ionization techniques.)

Figure 7 shows the energetics of applying energy selective electron impact ionization to photodissociation. We adjust the electron energy to be between the ionization potential of that fragment we wish to probe $[IP(A)]$ and the appearance potential of the fragment from the precursor molecule $[AP(A)]$ so as to observe signal at the mass of A^+ that comes only from the photofragment. Because the ion detection is mass selective, this is a means of identifying the primary photofragments using a universal detection scheme. The energetic discrimination shown in Figure 7 applies to

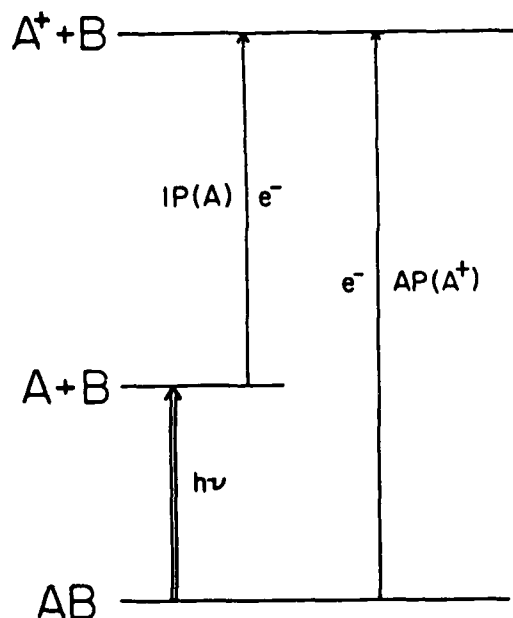


Figure 7

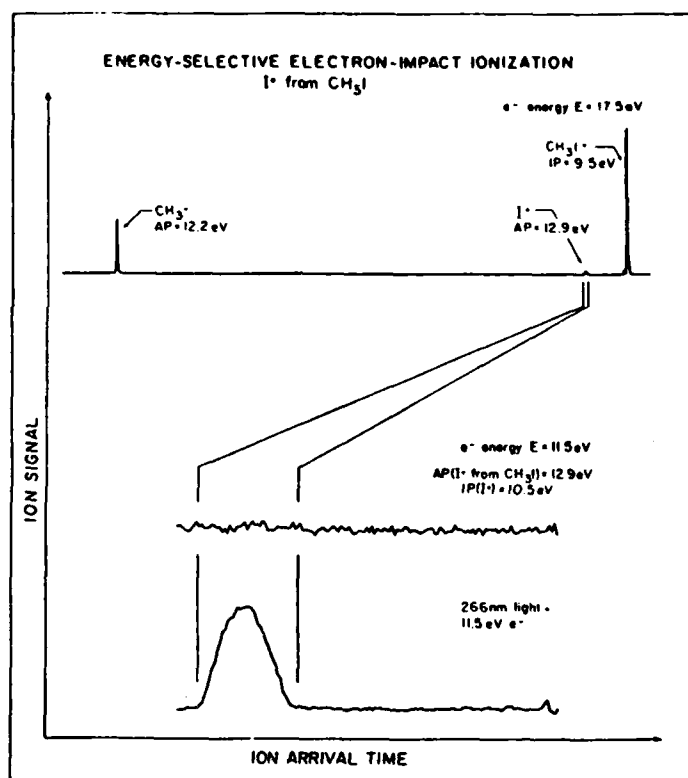


Figure 8

all systems in which the appearance potential of a fragment

exceeds the ionization potential of that fragment from the precursor molecule, a situation that obtains generally except for unusual cases where extensive fragment rearrangement makes the dissociation very exothermic. Because electron impact ionization is a general detection technique, we can study photodissociation processes that produce fragments that are impossible to detect by resonant laser ionization or laser induced fluorescence. The essential features of this approach are that the energy spread of ≈ 0.2 eV from our electron gun is considerably less than typical bond dissociation energies of 2 to 3 eV and that the electron gun operates efficiently at low electron energies. We have demonstrated this technique with CH_3I dissociation at wavelengths of 266 nm and 230 nm by detecting both the CH_3 fragment and the I fragment.²⁹ Figure 8 shows that we detect no I^+ above the background level when the electron energy is less than the appearance potential of I^+ from CH_3I unless we first photodissociate CH_3I to produce I (lower curve).

Energy selective electron impact ionization combined with time-of-flight mass spectrometry provides information about the disposal of energy into relative translation as well. Fragments that recoil toward the detector arrive sooner than those with no component of momentum in that direction while those that recoil away arrive later. Although this time difference is a small fraction of the total flight time, we can easily detect it in the shapes of the mass peaks. Figure 9 shows arrival time distributions of the iodine ions from electron impact ionization of the iodine atoms formed in the photolysis of CH_3I at 266 nm (upper

panel) and 230 nm (lower panel). Each panel shows the distribution for the photolysis laser being polarized along

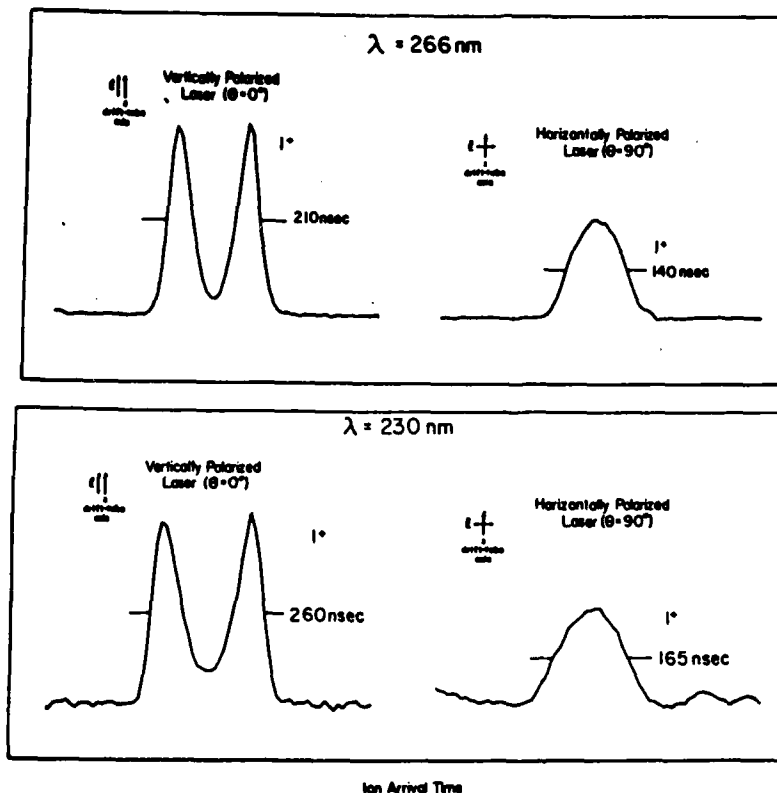


Figure 9

(vertical) or at a right angle (horizontal) to the axis of the flight tube in the mass spectrometer. The shapes of the features are exactly analogous to those obtained in Doppler scanning of transitions.³² Our technique and analysis approach is quite similar, except for minor technical details about mass spectrometer operation, to one developed contemporaneously by Houston and coworkers³³ using resonant multiphoton ionization of the fragments. The effect of kinetic energy release is most apparent for the laser polarized along the flight tube axis (left hand side of the figure). The separation of the two-maxima yields the kinetic energy release, which is the same at 266 nm as found

in angularly resolved photofragmentation experiments^{34,35} and is about 60% larger for 230 nm photolysis.

The shape of the features also carries information about the anisotropy of the recoil distribution, and our measurement at 230 nm is the first determination at that wavelength. Our value of the anisotropy parameter at 230 nm, $\beta=1.6$, shows that the transition is predominantly parallel.²⁹ We are able to conclude that the entire absorption band is dominated by a parallel transition, in disagreement with a deconvolution of magnetic circular dichroism data.³⁶ Because we collect all of the ions, we are able to work at lower laser fluences than required in fully angularly resolved experiments, but this sensitivity comes at the price of a reduction in the resolution of the recoil energy distribution. The potential of this approach lies in its ability to identify primary photofragmentation products by universal detection and to provide an assessment of the kinetic energy release at many different photolysis wavelengths.

References

1. T. R. Rizzo, C. C. Hayden, and F. F. Crim, J. Chem. Phys. 81, 4501 (1984).
2. T. M. Ticich, T. R. Rizzo, H.-R. Dübal, and F. F. Crim, J. Chem. Phys. 84, 1508 (1986).
3. L. J. Butler, T. M. Ticich, M. D. Likar, and F. F. Crim, J. Chem. Phys., 85, 2331 (1986).
4. A. Sinha, R.L. Vander Wal, and F.F. Crim, J. Chem. Phys. (to be published).
5. E. S. McGinley and F. F. Crim, J. Chem. Phys. 85, 5748 (1986).
6. E. S. McGinley and F. F. Crim, J. Chem. Phys. 85, 5741 (1986).
7. F.F. Crim, Annu. Rev. Phys. Chem. 35, 667 (1984).
8. H.-R. Dübal and F. F. Crim, J. Chem. Phys. 83, 3863 (1985).
9. T.M. Ticich, M.D. Likar, H-R. Dübal, L.J. Butler, and F.F. Crim, J. Chem. Phys. 87, 5820 (1987).
10. L. Brouwer, C.J. Cobos, J. Troe, H-R. Dübal, and F.F. Crim, J. Chem. Phys. 86, 6171 (1987).
11. T. Uzer, J.T. Hynes, and W.P. Reinhardt. Chem. Phys. Lett. 117, 600 (1985); J. Chem. Phys. 85, 5791 (1986).
12. F.F. Crim, in Molecular Photodissociation Dynamics, ed. J. Baggott and M. Ashfold (Royal Society of Chemistry, 1987) p. 177-210.
13. P. Pechukas and J.C. Light. J. Chem. Phys. 42, 3281 (1965); P. Pechukas and J.C. Light, and C. Rankin. J. Chem. Phys. 44, 794 (1966).
14. M. Quack and J. Troe. Ber. Bunsenges. Phys. Chem. 78, 240 (1972).
15. H. Reisler and C. Wittig, Annu. Rev. Phys. Chem. 37, 307 (1986).
16. C.B. Moore, Ber. Bunsenges. P. Chem. (to be published); Symposium on the Chemistry and Photophysics of Energetic Species, September, 1987.

17. I. Nadler, M. Noble, H. Reisler, C. Wittig, J. Chem. Phys. 82, 2608 (1985); C.X.W. Qian, M. Noble, I. Nadler, H. Reisler, and C. Wittig, J. Chem. Phys. 83, 5573 (1985).
18. A. Sinha, R.L. Vander Wal, L.J. Butler, and F.F. Crim, J. Phys. Chem. 91, 4645 (1987).
19. M.D. Likar, J.E. Baggott, A. Sinha, R.L. Vander Wal, and F.F. Crim, Faraday Transactions, 1988 (in press)
20. P.R. Stannard and W.M. Gelbart, J. Phys. Chem. 85, 3592 (1981).
21. M.L. Sage and J. Jortner, Adv. Chem. Phys. 47, 293 (1981). D.F. Heller and S. Mukamel, J. Chem. Phys. 70, 463 (1979).; Picosecond Phenomena, ed. C.V. Shank, E.P. Ippen, and S.L. Shapiro. New York: Springer, 1978, p. 51.
22. M.D. Likar, T.M. Ticich, A. Sinha, and F.F. Crim (to be published).
23. K.-H. Gericke, S. Klee, F.J. Comes and R.N. Dixon, J. Chem. Phys. 85, 4463 (1986).
24. M.P. Docker, A. Hodgson and J.P. Simons, Faraday Discuss. Chem. Soc. 82, 163 (1986).
25. G. Ondrey, N. van Veen and R. Bersohn, J. Chem. Phys., 78, 3732 (1983).
26. A. Jacobs, K. Kleinermaans, H. Kuge, and J. Wolfrum, J. Chem. Phys. 79, 3162 (1983).
27. M.D. Likar, A. Sinha, T.M. Ticich, R. Vander Wal, and F.F. Crim, Ber. Bunsenges. Phys. Chem., 1988 (in press).
28. J. August, M. Brouard, M.P. Docker, A. Hodgson, C.J. Milne, and J.P. Simons, Ber. Bunsenges. P. Chem. (1988) (in press).
29. S.M. Penn, C.C. Hayden, K.J. Carlson, and F.F. Crim, J. Chem. Phys., 1988 (submitted).
30. S.M. Penn, Ph.D. Thesis, University of Wisconsin, 1987.
31. C.C. Hayden, S.M. Penn, K.J. Carlson, and F.F. Crim, Rev. Sci. Instrum. (to be submitted).
32. R. Schmiedl, H. Dugan, W. Meier, and K.H. Welge, Z. Phys. A 304, 137 (1982).
33. R. Ogorzalek Loo, G.E. Hall, H.-P. Haerri, and P.L. Houston, J. Phys. Chem. (in press).

34. S.J. Riley and K.R. Wilson, Faraday Disc. Chem. Soc. 53, 132 (1972).
35. R.K. Sparks, K. Shobatake, L.R. Carlson, and Y.T. Lee, J. Chem. Phys. 75, 3838 (1981).
36. A. Gedanken and M.D. Rowe, Chem. Phys. Lett. 34, 39 (1975).

Publications Acknowledging ARO Support

1. Overtone Vibration Initiated Unimolecular Reaction of Tetramethyldioxetane in a Free Jet Expansion: A Comparison with RRKM Theory. E. S. McGinley and F. F. Crim, J. Chem. Phys. 85, 5748 (1986).
2. Unimolecular Reaction Rate Measurements for Molecules with Excited Overtone Vibrations. E.S. McGinley, L.J. Butler, T.M. Ticich, M.D. Likar, and F.F. Crim, J. Chim. Phys., 84, 393 (1987).
3. The Dissociation of Highly Vibrationally Excited Molecules. F.F. Crim, Molecular Photodissociation Dynamics, ed. J. Baggott and M. Ashfold (Royal Society of Chemistry, 1987) p. 177.
4. Two-Color Vibrationally Mediated Photodissociation of Nitric Acid. A. Sinha, R.L. Vander Wal, L.J. Butler, and F.F. Crim, J. Phys. Chem. 91, 4645 (1987).
5. Spectroscopy and Photodissociation Dynamics of Highly Vibrationally Excited Molecules. M.D. Likar, A. Sinha, T.M. Ticich, R. Vander Wal, and F.F. Crim, Ber. Bunsenges. Phys. Chem. 92, 289 (1988).
6. Vibrationally Mediated Photodissociation. M.D. Likar, J.E. Baggott, A. Sinha, R.L. Vander Wal, and F.F. Crim, Faraday Transactions, (1988) (in press).
7. Vibrational Overtone Spectroscopy of $H_2O(4\nu_{OH})$ Using Energy-Selective Electron Impact Ionization, C.C. Hayden, S.M. Penn, K.J. Carlson, and F.F. Crim, J. Phys. Chem. 92, 1397 (1988).
8. The Photodissociation of Methyl Iodide at 229.4 nm: A Determination of the Fragment Recoil Anisotropy using Energy-Selective Electron Impact Ionization and Time-of-Flight Mass Spectrometry, S.M. Penn, C.C. Hayden, K.J. Carlson Muyskens, and F.F. Crim, J. Chem. Phys. 89, 2909 (1988).

Participating Scientific Personnel

Dr. L.J. Butler	(research associate)	
Dr. C.C. Hayden	(research assistant)	
Dr. Amitabha Sinha	(research associate)	
K.J. Carlson	(research assistant)	
L.G. Huey	(research assistant)	
S.M. Penn	(research assistant)	Ph.D. (1987)
R.L. Vander Wal	(research assistant)	